Int. J. Electrochem. Sci., 13 **(2018)** 2860 – 2874, doi: 10.20964/2018.03.05

International Journal of
ELECTROCHEMICAL
SCIENCE
www.electrochemsci.org

Magnetron Sputtering Silicon Thin Film Electrodes for Lithium-Ion Batteries

E. Evshchik[1,*], *D. Novikov*[2], *A. Levchenko*[1,2], *S. Nefedkin*[3], *A.V. Shikhovtseva*[1], *O.V. Bushkova*[1,2,4], *Yu. A. Dobrovolsky*[1]

[1] Institute of Problems of Chemical Physics of Russian Academy of Sciences, pr. akad. Semenova 1, Chernogolovka, Russia
[2] Inenergy LLC, Elektrodnajast. 12, Bld. 1, Moscow, Russia
[3] MEI National Research University, 14, Krasnokazarmennaya, Moscow, Russia
[4] Institute of Solid State Chemistry, Ural Branch of the Russian Academy of Sciences, Pervomaiskaya st. 91, Ekaterinburg, Russia
[*]E-mail: liza@icp.ac.ru

Received: 23 October 2017 / *Accepted:* 19 December 2017 / *Published:* 5 February 2018

Thin silicon films were deposited on surface-modified copper foil by magnetron sputtering; Si mass loading varied from 0.013 to 0.400 mg/cm. Scanning electron microscopy (SEM), X-ray photoelectron spectroscopy (XPS), X-ray diffraction (XRD), and transmission electron microscopy (TEM) were used to characterize the structure, morphology, and composition of the Si films as a function of mass loading. It was established that Si films repeated the hill-like morphology of Cu foil surface and consisted of nearly spherical agglomerates of amorphous silicon; the average size and packing of agglomerates varied as the Si mass loading changed. Galvanostatic half-cell electrochemical measurements were carried out within the range of 0.04–2.0 V with a lithium foil as the counter electrode and 1M solution of $LiPF_6$ in 1:1 (v/v) mixture of ethylene carbonate (EC) and diethyl carbonate (DEC) as the electrolyte. According to the results obtained, the highest value of the reversible capacity of about 1200 mAh/g after 50 charge-discharge cycles at 0.1 *C* was observed in the electrodes with a Si mass loading of 0.293 mg/cm. The non-monotonic dependence of the reversible capacity *vs.* Si mass loading is likely to be caused by the structural evolution of the amorphous Si thin films.

Keywords: Li-ion batteries, Silicon electrode, Thin film, Magnetron sputtering, Morphology, Cycling performance

1. INTRODUCTION

Silicon has the highest theoretical capacity among negative electrode materials of lithium-ion batteries [1-6]. At room temperature, silicon electrode capacity can reach the value of 3590 mAh/g,

which corresponds to the formation of $Li_{15}Si_4$ alloy; this is far above the theoretical capacity of graphite (372 mAh/g) commonly used in commercial lithium-ion batteries. However, silicon electrodes are known to be easily destroyed during lithium insertion/extraction due to significant volume changes (up to 300%). It leads to pulverization of silicon particles and loss of electrical contact with the current collector and consequently to the electrode capacity fading [1-6].

Nano-sized silicon materials with different architectures may be resistant to mechanical failure in case of multiple insertion/extraction of Li and can significantly improve Li transport, as demonstrated by numerous studies (e.g., [7-27]) and summarized in recent reviews [1-6]. However, their preparation techniques are often complicated and very expensive, which limits the use of such materials in commercial batteries. Among them, thin film growth techniques based on various deposition methods are the most practicable, and thin-film electrodes themselves have several advantages over bulk materials in Li-ion batteries, as it was emphasized in [9, 18]: they usually ensure better stability and capacity retention, operate kinetically faster due to shorter pathways for Li^+ insertion/extraction, and demonstrate high specific capacities. The most common methods to obtain thin silicon films are magnetron sputtering [7, 9, 10, 18, 21, 25-28], thermal evaporation [12, 14, 15, 16, 29], and vapor deposition [11, 13, 17, 30]. Among them, magnetron sputtering seems to be very promising due to the ease of its use; in addition, this method ensures good adhesion between particles and the current collector substrate due to the Si/Cu interdiffusion [7, 21, 26].

It was found that changes in the film thickness affect the electrochemical behavior of the silicon film noticeably. Regretfully, there are very few studies that have investigated the correlation between the thickness of the Si film obtained by magnetron sputtering and the cycling performance of such electrodes [7, 9, 21, 25, 26]. Therefore, no clear understanding of the influence of the film thickness and structure on the specific capacity and cyclability, as well as on irreversible processes resulting in the Si film degradation, was achieved.

In this contribution, we investigated the structural and electrochemical properties of thin silicon films deposited by magnetron sputtering on surface-modified Cu foil, as a function of Si mass loading (0.013 to 0.400 mg/cm). Scanning electron microscopy (SEM), X-ray photoelectron spectroscopy (XPS), X-ray diffraction (XRD), and transmission electron microscopy (TEM) were used to characterize the structure and morphology of the Si films. It was established that the electrochemical performance of a Si film is dependent on the Si mass loading in a complicated way due to their structural evolution. The morphological changes of a thin silicon film during long-term electrochemical cycling were also studied.

2. EXPERIMENTAL

2.1. Preparation of silicon films by magnetron sputtering

Silicon thin films were prepared by RT magnetron sputtering (CROWDION-M1 instrument (LLC Ionteks, Russia) from a commercial Si target (99.999%). The distance from the target to the Cu foil substrate was 100 mm, which ensured uniform silicon coating. The sputtering process was performed at the magnetron frequency of 13.56 MHz. The current value was maintained at 0.15 A

under 440–450 V. High-purity argon was used as a working gas under a pressure of 6.7 Pa. Si mass loading varied from 0.013 to 0.400 mg/cm^2 depending on the time of the deposition process.

The surface-modified copper foil with a thickness of 50 μm was used as the substrate; the foil was provided by the JSC Special Design-and-Technology Bureau for electrochemistry (Moscow, Russia).

2.2. Physicochemical characterization of silicon thin films

The study of the thin silicon films' structure and morphology was carried out by scanning electron microscopy (Zeiss LEO SUPRA 25, Germany), as well as transmission electron microscopy (JEOL JEM-2100, Japan). To perform TEM measurements, the Si film was separated from the Cu substrate and then deposited on a carbon grid from ethanol suspension. X-ray patterns of Si films were obtained with a Rigaku D-MAX–2200 V diffractometer with a vertical goniometer (Cu $K_{\alpha 1}$ radiation, 2Θ = 5–90^o). XRD and microdiffraction data were analyzed using the ICDD-JCPDS database. The mass loading density of the obtained Si films was determined gravimetrically. The chemical composition of the Si film surface was established by X-ray photoelectron spectroscopy (Omicron Multiprobe RM, UK). The binding energy scale of the spectrometer was preliminarily calibrated by the position of the peaks of Au $4f_{7/2}$(83.96 eV) and Cu $2p_{3/2}$ (932.62 eV) core levels for pure gold and copper metals. The spectra were collected in the constant analyzer energy mode with 40 eV pass energy. The chemical states of Si atoms were determined by analyzing the Si2*p* line, using reference spectral data [31] along with the data of publications [32-35].

2.3. Electrochemical measurements

The electrochemical properties of Si thin films on a Cu substrate were studied using sealed Teflon three-electrode cells of flat-parallel design. The cells contained a working electrode with the active surface of 2.25 cm^2, a lithium counter-electrode, and a lithium reference electrode. The electrodes were separated with a porous polypropylene film PORP (Ufim, Russia), impregnated with a liquid electrolyte. The solution of 1M of $LiPF_6$ in an ethylene carbonate and diethyl carbonate mixture (1:1, v/v) was used as the electrolyte; all components were supplied by Sigma Aldrich. The residual water content in the electrolyte solution did not exceed 30 ppm. The electrochemical cells were assembled within an argon-filled MBraun glove box where moisture and oxygen levels were maintained at less than 0.1 ppm.

The galvanostatic charge/discharge cycling of the electrochemical cells was performed in the voltage range of 0.04–2.0 V *vs.* Li/Li$^+$ at 0.1 *C* rate using P-20X80 multichannel potentiostat (Elins, Russia). The gravimetric capacity was calculated using the mass loading of the films. After cycling, the cells were carefully disassembled, and the working electrodes were removed and thoroughly rinsed with dimethoxyethane inside a glove box. The samples thus obtained were then examined with an electron microscope. The rate of the cyclic voltammogram registration with the same equipment was 0.01 mV/s.

3. RESULTS AND DISCUSSION

3.1 Characterization of silicon thin films prepared by magnetron sputtering

Roughening the electrode substrate for silicon deposition is found important to ensure better cycling performance. Rough foil effectively increases the contact area and enhances adhesion between the Si film and the current collector, which makes the whole electrode more resistant to volume changes and helps the active Si material to maintain the electronic contact with the foil during charging and discharging [1, 11, 14, 15, 18, 25, 27, 29]. Therefore, in the present work, surface-modified copper foil was used as the substrate for Si films' deposition by magnetron sputtering. Figure 1 shows the SEM images of the used copper foil's surface and cross-section. A pyramid-like morphology with small rounded particles (≤1μm in diameter) on the surface of protuberances can be identified in the figure; such a morphology provides a large surface area for the subsequent Si deposition process.

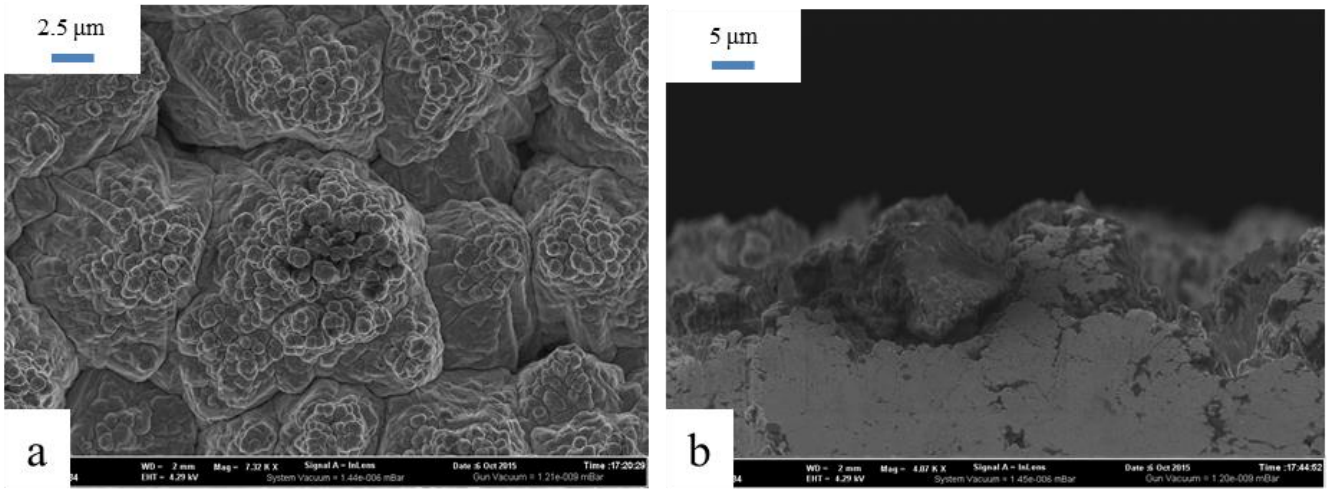

Figure 1. SEM images of the copper foil surface (a) and cross-section (b)

The SEM images of the Si films with a mass loading of 0.013, 0.293, and 0.400 mg/cm^2 obtained by magnetron sputtering on the Cu foil substrate are shown in Figure 3. As can be seen, the deposited silicon has completely covered the Cu foil protuberances, and the film's morphology obviously changes as the Si mass loading alters. At the lowest value, 0.013 mg/cm^2, the Si film fully repeats the complex relief of the Cu-foil substrate (Fig. 2a). Further magnification (Fig. 2b) allows observing rounded agglomerates with an average size of ~100-400 nm, composed of nano-sized spherical silicon grains. The agglomerates form a close-packed continuous Si layer. The thickness of this film was estimated at ~55 nm, assuming that the silicon density is 2.33 g/cm^3. It should be noted that this is an overestimated thickness value since the geometric area of the Si film was used in these calculations disregarding the complex relief of the Cu substrate.

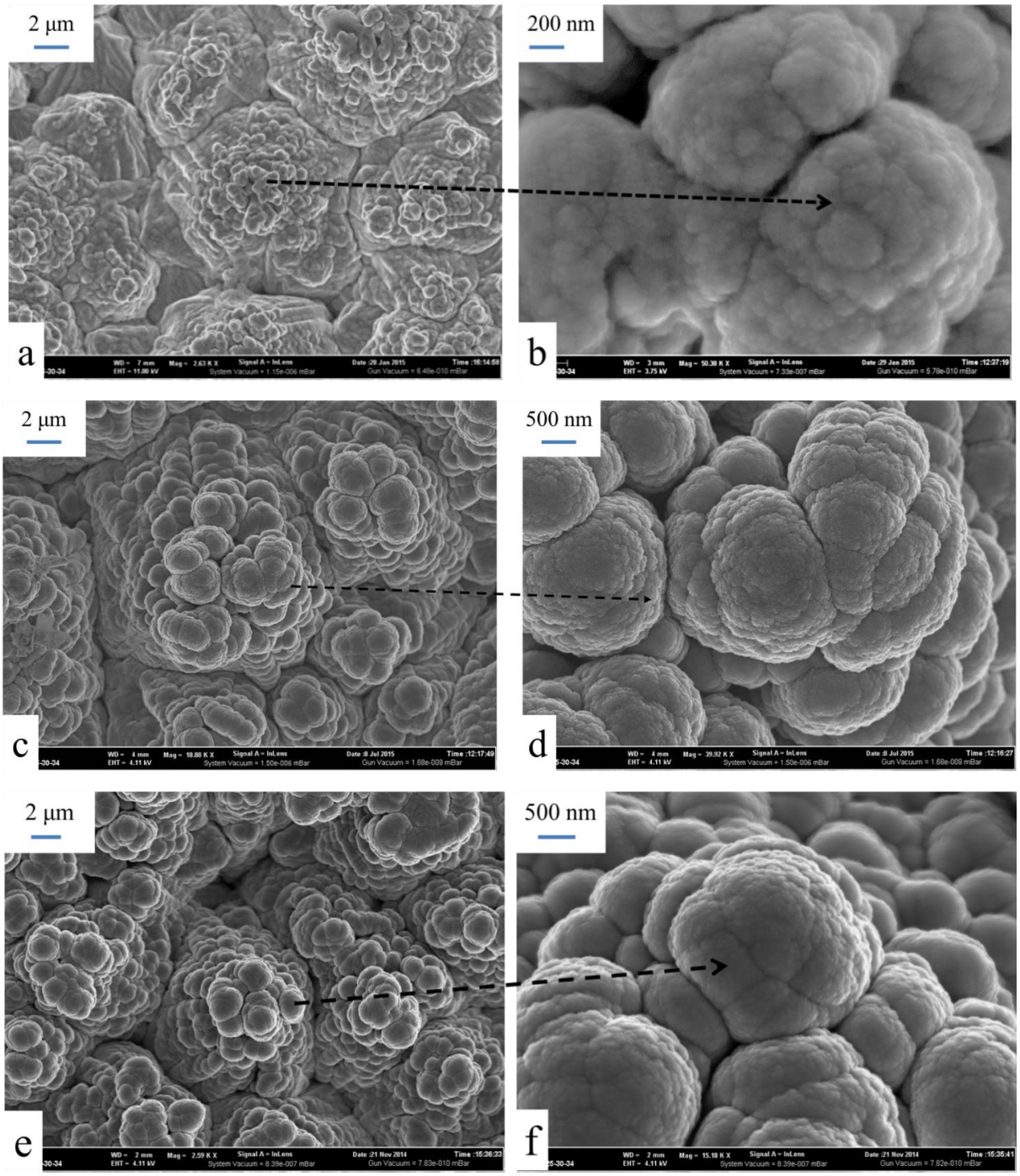

Figure 2. SEM images of silicon thin films with 0.013 (a, b), 0.293 (c, d) and 0.400 (e, f) mg/cm^2 mass loading

At a higher Si mass loading, 0.293 and 0.400 mg/cm^2 (corresponding to the film thickness of approximately 1200 and 1700 nm, respectively), micro-grains on the protuberances' surface of the Cu-foil substrate are fully overlapped by large spherical silicon agglomerates forming a continuous silicon film as evident from Fig. 2c and e. These Si agglomerates have an average size of around 1-2 µm (Fig. 2d and f), which is noticeably higher than those shown in Fig. 2a and b. As can be identified from Fig. 2d and f, the large silicon agglomerates, in turn, consist of smaller agglomerated particles. The Si film

with the highest mass loading, 0.400 mg/cm^2 (Fig. 2e and f), is characterized by a closer packing of large silicon agglomerates, which however reproduces the complex hill-like relief of the copper substrate.

It is worth noting that the hill-like relief of the Cu-foil substrate determines the features of the architecture of deposited Si films, which follow its complex relief thus forming a large surface area. It provides a considerable room for the silicon particles' volume expansion upon lithiation and may enhance the structural stability of electrode. Moreover, the packing of round silicon agglomerates causes formation of numerous micro- and nanopores within the silicon layer, ensuring high permeability of the electrode surface for the electrolyte solution, in contrast to solid non-porous films, and minimizing diffusion limitations during the lithiation/delithiation processes.

The formation of a continuous film composed of close-packed round agglomerates seems to be typical for silicon deposited on a surface-modified copper foil by magnetron sputtering (see, for example, [21, 25, 27]).

In order to determine the atomic arrangement within silicon films, more detailed characterization by transmission electron microscopy was used. Figure 3 shows the TEM image for a fragment of a silicon film with a mass loading of 0.293 mg/cm^2 obtained by the magnetron sputtering along with electron diffraction ring patterns for selected areas of the sample. The boundary between the silicon film and the carbon substrate used for TEM is clearly visible as can be seen in the high-resolution micrograph (Fig. 3a). Taking into account the TEM data, we can assume the existence of 5-10 nm size particles, which form silicon agglomerates observed in SEM images (Fig. 2).

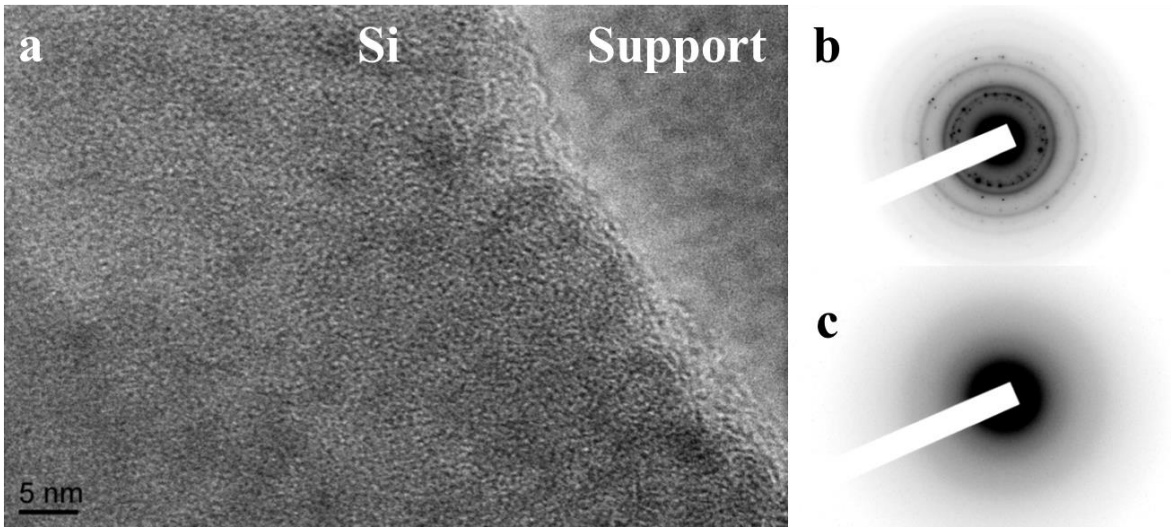

Figure 3. TEM micrograph (a) of a fragment of the silicon film with mass loading of 0.293 mg/cm^2 on a carbon substrate along with microdiffraction rings for selected areas of the sample (b, c)

It is difficult to find the ordered crystalline lattice in high-resolution TEM image (Fig. 3a); one can assume therefore that silicon film is mostly amorphous. The conclusion agrees well with the results of X-ray diffraction for silicon films under study: all peaks in their XRD patterns (not shown) were attributed to the Cu foil substrate only. However, the microdiffraction patterns show very

diffusing rings (Fig. 3c) or even rather sharp rings and dark spots (Fig. 3b), which suggests that the film is not totally amorphous; a short-range ordering may exist on the atomic scale along with crystalline phases. It must be emphasized that the microdiffraction patterns presented in Fig. 3b and c are typical; the same results were obtained for silicon films with other mass loading values, deposited on Cu foil by magnetron sputtering.

Interplanar distances (d) estimated from the microdiffraction pattern presented in Fig. 3b are given in Table 1; it is easy to see that crystalline reflexes must be attributed to silicon dioxide nanocrystals.

In order to obtain more information on the chemical composition of the Si film surface, we performed XPS measurements. The analysis of the photoelectron spectrum over a wide range of binding energy E_b showed the presence of silicon and oxygen; the signal from the copper substrate was also registered.

Table 1. Interplanar distances calculated from the microdiffraction pattern presented in Fig. 3b in comparison with reference data from ICDD-JCPDS

d (Å)	SiO_2 (card No. 46-1045)		Si (card No. 27–1402)	
	$h\,k\,l$	d (Å)	$h\,k\,l$	d (Å)
2.47	110	2.4569	111	3.1354
2.13	200	2.1277	220	1.9200
1.51	211	1.5415	311	1.6374
1.37	301	1.3719	4000	1.3577
1.22	220	1.2283	331	1.2459

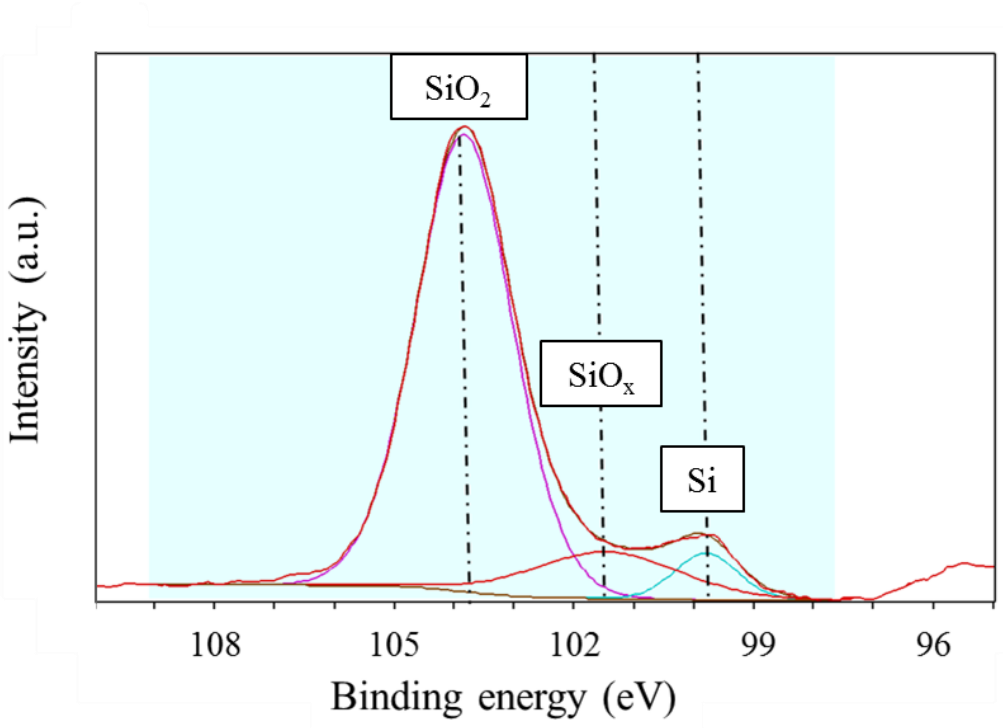

Figure 4. Si2p spectrum of the surface of a silicon film obtained by the magnetron sputtering

The typical Si2p spectrum of a silicon film is shown in Figure 4. Deconvolution of the XPS spectra revealed the peak at 99.7 eV, which was assigned to pure silicon (Si-Si bonds); the other peaks at 101.7 and 103.2 eV were attributed to SiO_x and SiO_2, respectively, in accordance with Refs. [31-35]. The XPS results showed that more than 90% of the silicon atoms on the film surface form SiO_2.

Thus, the findings of SEM, TEM, XPS, XRD and microdiffraction study lead to conclusion that silicon films obtained by magnetron sputtering on a Cu-foil substrate are composed of amorphous silicon with short-range ordering and a thin nanocrystalline SiO_2 layer on the Si film's surface. The amorphous state of silicon is in good agreement with reference data for Si films deposited on Cu foil by magnetron sputtering [7, 9, 18, 21, 25-28]. A nano-scale layer of silicon dioxide on the surface of a nanostructured silicon material can ensure greatly enhanced overall electrochemical performance due to its roles of a barrier and structural buffer (see, for example, [24] and references therein).

3.2 Electrochemical performance of silicon thin-film electrodes

Cyclic voltammograms (CV) for a silicon thin-film electrode on a Cu foil substrate with 0.293 mg/cm^2 mass loading are given in Figure 5. It should be mentioned that peaks become more pronounced as the number of cycles increases. Three cathode (E = 0.41 V, 0.13 V, and 0.04 V) and two anode (E = 0.35 V and 0.48 V) peaks were observed on the CV of any stable cycle (as the example, the 10th cycle is shown in Fig. 5). Cathode peaks can be attributed to insertion of lithium into the amorphous silicon structure whereas anode ones refer to extraction of Li from silicon. According to [36], the cathode peak at 0.41V corresponds to the $Li_{0\text{-}0.39}Si_{5/22}$ phase formation with a pseudo-thermodynamic potential of 0.35 V in the calculated charging curve. The peak at 0.13V corresponds to the formation of the $Li_{0.52\text{-}0.74}Si_{5/22}$ phase with a pseudo-thermodynamic potential of 0.14 V. The last cathode peak at 0.04 V corresponds to the $Li_{0.74\text{-}1.0}Si_{5/22}$ phase [36].

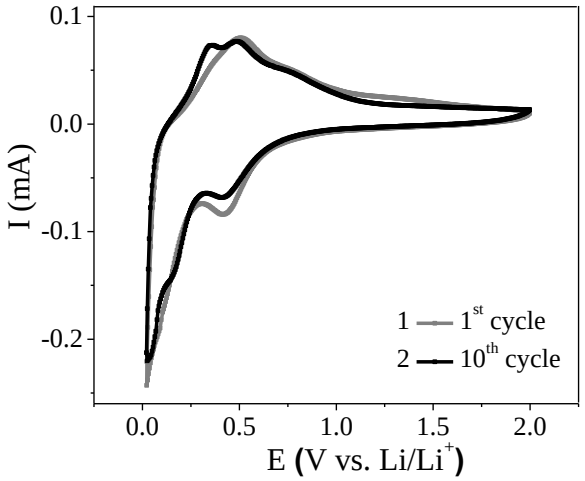

Figure 5. Cyclic voltammograms for silicon film with 0.293 mg/cm^2 mass loading (scanning rate 0.1 mV/s)

The difference between the peak potentials of the anodic and cathodic branches of the voltammograms is small; this indicates a relatively low kinetic polarization and low internal resistance of silicon thin-film electrodes. The fact can be explained by the features of the thin Si film's structure discussed above (Section 3.1).

An example of cycling performance of a thin silicon film deposited on a surface-modified Cu foil by magnetron sputtering is shown in Figure 6. The charge/discharge curves of the lithium insertion/extraction into Si demonstrated a classical shape as evident from Fig. 6. For all silicon films under investigation, the shape of the charge/discharge curves was almost the same (except for the first cycle), and they did not change during the cycling.

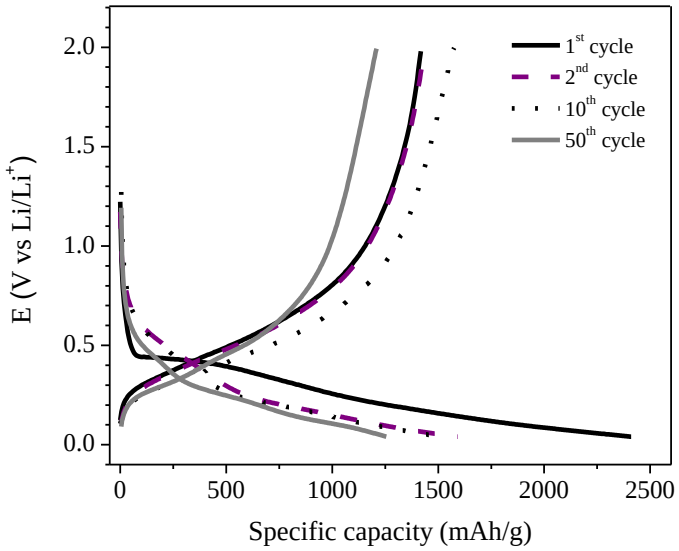

Figure 6. Voltage profiles of silicon thin-film electrode with mass loading of 0.293 mg/cm^2 at 0.1 *C* rate for first, second, 10th and 50th cycles

The quantity of electricity in the first cathodic half-cycle (lithiation) exceeds this value in the first anodic half-cycle (delithiation); the difference characterizes the irreversible capacity, which is attributed to the well-known electrochemical process of formation of a solid electrolyte interface (SEI) on the silicon surface. Irreversible capacity values for Si films can be found in Table 2 along with other cycling parameters. The highest value of irreversible capacity (about 2743 mAh/g) in the first cycle was observed for the electrode with the smallest mass loading, 0.013 mg/cm^2, and the lowest one, 562 mAh/g, for the greatest mass loading, 0.400 mg/cm^2. The fact can be attributed to the substantial difference in the microstructure of these films (see Fig. 2). It is important to mention that for the thinnest silicon film with 0.013 mg/cm^2 mass loading, the quantity of electricity in the first cathodic half-cycle was 4720 mAh/g, which substantially exceeds the theoretical value of room-temperature silicon's capacity, 3590 mAh/g. This implies that this film has a very large and very active surface available for electrolyte solution, which facilitates irreversible side electrochemical processes such as reduction of electrolyte components. Indeed, SEM images of the film confirm this assumption (Fig. 2a

and b). As cycling continues, the irreversible capacity decreases but not to zero; the smallest value of 11 mAh/g was obtained after 50 cycles for the sample with 0.112 mg/cm^2 mass loading (Table 2).

Table 2. Cycling parameters for Si thin-film electrodes with different mass loading in anode half-cells

Mass loading (mg/cm^2)	Irreversible capacity (mAh/g)		Discharge capacity (mAh/g)		Coulombic efficiency (%)		Capacity retention (%)
	1st cycle	50th cycle	1st cycle	50th cycle	1st cycle	50th cycle	
0.013	2743	59	1991	213	42	78	11
0.033	785	39	897	488	53	92	54
0.112	847	11	578	193	40	94	33
0.293	992	46	1418	1208	58	96	85
0.400	562	75	2634	324	82	81	12

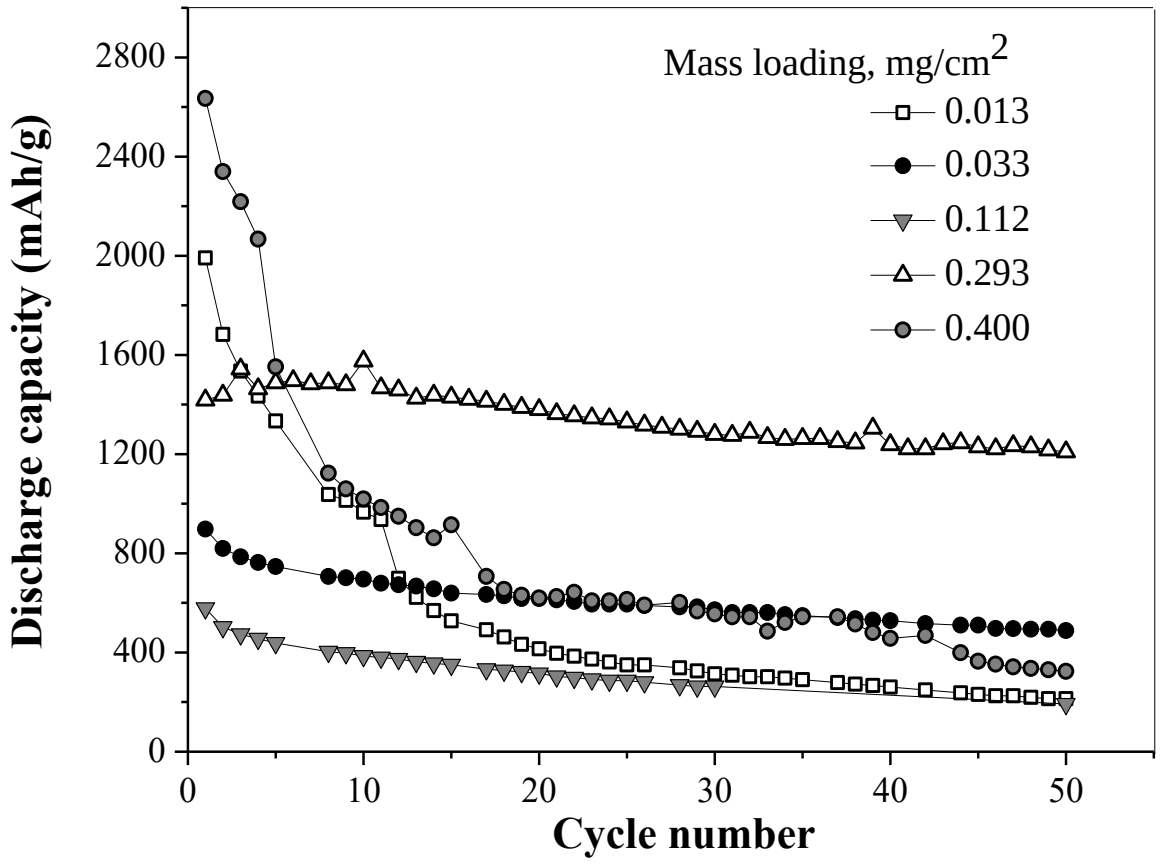

Figure 7. Cycle-life performance for the Si thin-film electrodes with different mass loading deposited on surface-modified Cu foil

The discharge (delithiation) capacity evolution during long-term galvanostatic cycling of Si thin-film electrodes with different mass loading is shown in Figure 7 and Table 2. As can be seen, the highest values of the discharge capacity in the first cycle, 2634 and 1991 mAh/g, were observed for the thickest and thinnest Si films with a mass loading of 0.013 and 0.400 mg/cm^2, respectively. Both samples quickly degraded as the cycling proceeded, but the degradation rate of the films significantly reduced after the initial drop of capacity, as we can see from Fig. 7. The most stable cycling behavior with the highest discharge capacity of ~1200 mAh/g after the 50th cycle was observed for the sample with mass loading of 0.293 mg/cm^2 (Fig. 7).

The discharge capacity as a function of mass loading for Si thin-film electrodes deposited on a Cu foil is shown in Figure 8 for the 1st, 5th and 50th cycles. One can see that as cycling performance of Si thin-film electrodes stabilized (the 50th cycle), two maximums appeared in the curve. The first one, relatively small in its value, corresponds to the mass loading of 0.033 mg/cm^2 while the second one is at the 0.293 mg/cm^2 mass loading. It should be noted that the minimum values at any cycle number were observed for the film with mass loading of 0.112 mg/cm^2. Upon that, all three samples mentioned above demonstrated rather high coulombic efficiency during the 50th cycle (≥92%), with the highest one for the sample with 0.293 mg/cm^2 mass loading (96%).

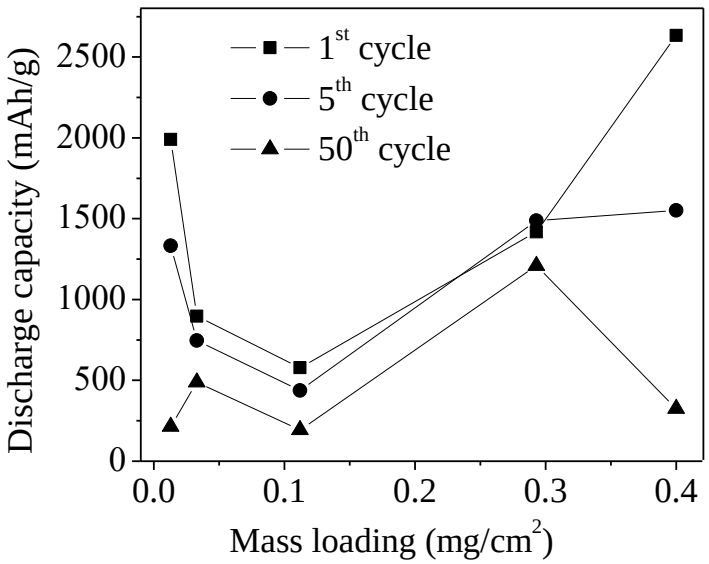

Figure 8. Discharge capacity of the Si thin-film electrodes deposited on Cu foil as a function of mass loading for the 1st, 5th and 50th cycles

The non-monotonous dependence of discharge capacity on mass loading (i.e., film thickness) seems to be intrinsic to thin silicon films deposited on metal foil substrate. Indeed, it is easy to conclude from reference data (see, for example, [7, 24-26] and Table 2 in [9]) that the best cycling behavior was observed for Si films whose thickness values remained within two intervals, ~200-400 nm (data for thinner films were not found) and 1000-2000 nm. The upper limit is most likely due to the limitations of lithium diffusion into silicon. Taking into account the lithium diffusion coefficient in amorphous Si equal to 10^{-16} m^2/s approx., the diffusion length was estimated in [25] as 2000 nm for the

charging (lithiation) rate of 0.1 *C*. Therefore, silicon grains larger than this value cannot be fully lithiated during charging at 0.1 *C*. At a higher charging rate, 1 *C*, the diffusion length was estimated as 600 nm [25].

The two maximum discharge capacity values after 50 charge/discharge cycles revealed in the present work are equal to ~145 nm (mass loading 0.033 mg/cm^2) and ~1200 nm (0.293 mg/cm^2) (overestimated values, as discussed above), which nearly fall into these intervals. It seems that such values of the Si film thickness provide the morphology with the best availability of the Si electrode surface for the electrolyte and the highest integrity of Si films upon lithiation/delithiation. These two optimal thickness values nearly correspond to the average sizes of agglomerated particles forming the silicon layer on the Cu substrate surfaces (see Fig. 2 and comments in Section 3.1), ~100–400 nm and 1–2 μm. It is likely that such film morphology ensures both strong adhesion of silicon granules and numerous micropores, which facilitates the contact with the electrolyte solution and reduces the stress caused by volume expansion/contraction during the cycling. In addition, it removes the limitations of Li diffusion into Si.

The values of the discharge capacity for thin films obtained in this work are not inferior to those described in the literature as you can see from Table 3 where electrochemical properties of Si thin film anodes with different thickness are summarized.

Table 3. Characteristics of thin-film silicon electrodes produced by magnetron sputtering

Substrate	Thickness, nm	Initial capacity, mA/g	Cycle numbers	Discharge capacity (last cycle), mAh/g	Reference
Ni	1200	3300/3000	30	1200	26
Cu	1000-2000	3400/2300	30	1500	19
Cu	250	4100	30	3500	21
Cu	1000	3400	30	1200	21
Cu	200	3000	10	1500	7
Cu	275	2500	500	1500	28
Cu	300	2490	350	1400	37
Cu	90	2300	100	1000	38
Cu	87	3800	80	2700	39
Cu	~1200*	1418	50	1208	This work

* mass loading of 0.293 mg/cm^2

Figure 9 illustrates the changes in the morphology of the thin silicon film after 50 galvanostatic charge-discharge cycles. A comparison of SEM images with the 2-μm scale before (Fig. 2a) and after

(Fig. 9a) the cycling shows that the electrode surface remained almost unchanged; the Si film was not destroyed after multiple insertion and extraction of lithium. Further magnification (Fig. 9b) allows observing cracks appeared between the round silicon agglomerates, as well as signs of their surface etching.

In summary, it can be concluded that the special microstructure of the thin Si film obtained by magnetron sputtering helps the active material to accommodate a volume change and ensures rather high cycling stability after the initial 3 to 20 cycles (depending on the film thickness) when the surface transformations have almost been completed.

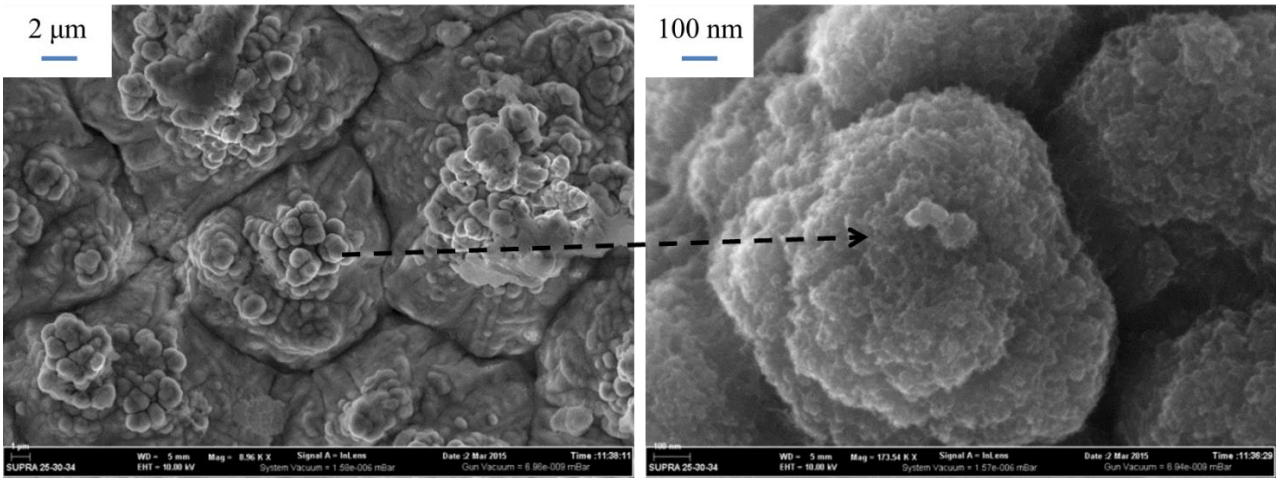

Figure 9. SEM images of silicon film on Cu-foil substrate (0.033 mg/cm^2 mass loading) after 50 galvanostatic charge-discharge cycles

4. CONCLUSIONS

The structure and electrochemical performance of the silicon thin films deposited on the structural-modified Cu foil by the magnetron sputtering were studied to investigate the influence of film thickness. The electrochemical properties indicate an optimal Si mass loading of 0.293 mg/cm^2 (corresponding to the film thickness of approximately 1200 nm) at which Si electrodes demonstrated the highest reversible capacity (~1200 mAh/g) and coulombic efficiency (96%) as well as the best cycling stability (capacity retention 96%). Non-monotonic dependence of the reversible capacity *vs.* Si mass loading is likely to be caused by the structural evolution of the amorphous silicon thin films.

ACKNOWLEDGEMENTS
This work was supported by Russian Science Foundation (grant No. 15-13-00166).

References

1. X. Zuo, J. Zhu, P. Müller-Buschbaum, Y.-J.Cheng, *Nano Energy*, 31 (2017) 113.

2. M. Ko, S. Chae, J. Cho, *ChemElectroChem* ,2(2015) 1651.
3. M. Ashuri, Q. He, L.L. Shaw. *Nanoscale*, 8 (2016) 103.
4. B. Liang, Y. Liu, Y. Xu. *Journal of Power Sources*, 267 (2014) 490.
5. J. R. Szczech, S. Jin, *Energy & Environmental Science*, 4 (2011) 56.
6. F. Ozanam, M. Rosso. Materials Science and Engineering, B (2016) 2.
7. T. Moon, C. Kim, B. Park, *J. Power Sources*, 155 (2006) 394.
8. H. Li, X. Huang, L. Chen, Z. Wub, Y.A. Liang, *Electrochem. Solid-State Lett.*, 2 (1999) 547.
9. M.T. Demirkan, L. Trahey, T. Karabacak, *J. Power Sources*, 273 (2015) 52.
10. T.L. Kulova, A.A. Mironenko, A.M. Skundin, A.S. Rudy, V.V. Naumov, D.E. Pukhov, *Int. J. Electrochem. Sci.*, 11 (2016) 1370.
11. M. Uehara, J. Suzuki, K. Tamura, K. Sekine, T. Takamura, *J. Power Sources*, 146 (2005) 441.
12. S. Ohara, J. Suzuki, K. Sekine, T. Takamura, *J. Power Sources*, 136 (2004) 303.
13. K. Yoshimura, J. Suzuki, K. Sekine, T. Takamura, *J. Power Sources*, 146 (2005) 445.
14. T. Takamura, M. Uehara, J. Suzuki, K. Sekine, K. Tamura, *J. Power Sources*, 158 (2006) 1401.
15. T. Takamura, S. Ohara, M. Uehara, J. Suzuki, K. Sekine, *J. Power Sources*, 129 (2004) 96.
16. S. Ohara, J. Suzuki, K. Sekine, T. Takamura, *J. Power Sources*, 119 (2003) 591.
17. M. Saito, T. Yamada, C. Yodoya, A. Kamei, M. Hirota, T. Takenaka, A. Tasaka, M. Inaba, *Solid State Ionics*, 225 (2012) 506.
18. J.K. Lee, J.-Y Jung, S.-W. Lee, H.-S. Moon, J.-W. Park, *J. Power Sources*, 129 (2004) 270.
19. K.-L. Lee, J.-Y. Jung, S.-W. Lee, H.-S. Moon, J.-W. Park, *J. Power Sources*, 130 (2004) 241.
20. V. V. Emets, T. L. Kulova, A. M. Skundin, *Int. J. Electrochem. Sci.*, 12 (2017) 2754.
21. J.P. Maranchi, A.F. Hepp, P.N. Kumta, *Electrochem. Solid-State Lett.*, 6 (2003) A198.
22. V. Baranchugov, E. Markevich, E. Pollak, G. Salitra, D. Aurbach, *Electrochem. Comm.*, 9 (2007) 796.
23. H. Yang, P. Fu, H. Zhang, Y. Song, Z. Zhou, M. Wu, L. Huang, G. Xu, *J. Power Sources*, 174 (2007) 533.
24. D.V. Novikov, E.Yu. Evshik, V.I. Berestenko, T.V. Yaroslavtseva, A.V. Levchenko, M.V. Kuznetsov, N.G. Bukun, O.V. Bushkova, Yu.A. Dobrovolsky, *Electrochem. Acta*, 208 (2016) 109.
25. F. Farmakis, C. Elmasides, P. Fanz, M. Hagen, N.Georgoulas, *Journal of Power Sources* , 293 (2015) 301.
26. J. P. Maranchi, A. F. Hepp, A. G. Evans, N. T. Nuhfer and P. N. Kumta,*J. Electrochem. Soc.*, 153(2006) 1246.
27. F. Paloukis, C. Elmasides, F. Farmakis, P. Selinis, S.G. Neophytides, N. Georgoulas, *Journal of Power Sources* , 331 (2016) 285.
28. L.B. Chen, J.Y. Xie, H.C. Yu, T.H. Wang, *J. Appl., Electrochem.*, 39 (2009) 1157.
29. T. Zhang, H.P. Zhang, L.C. Yang, B. Wang, Y.P. Wu, T. Takamura., *Electrochimica Acta*, 53 (2008) 5660.
30. H. Jung, M. Park, Y.-G. Yoon, G.-B. Kim, S.-K. Joo, *Journal of Power Sources* , 115 (2003) 346.
31. National Institute of Standards and Technology, The NIST X-Ray Photoelectron Spectroscopy (XPS) Database, Standard Reference Database 20, Version 4.1 (2012) https://srdata.nist.gov/xps/
32. N.I. Fainer, M.L. Kosinova, Yu.M. Rumyantsev, *The Journal of the Russian Chemical Society*, XLV (2001) 101.
33. X.L. Wu, Y. Gu, S.J. Xiong, J.M. Zhu, G.S. Huang, X.M. Bao, G.G. Siu, *J. Appl. Phys.*, 94 (2003) 5247.
34. M. Nakazawa, S. Kawase, H. Sekiyama, *J. Appl. Phys.*, 65 (1989) 4014.
35. J.-W. Song, C. C. Nguyen and S.-W. Song, *RSC Advances*, 2 (2012) 2003.
36. R. Chandrasekaran, A. Magasinski, G. Yushin, T.F. Fuller, *J. Electrochem. Soc.*, 157 (2010) A1139.
37. L.B. Chen, J.Y. Xie, H.C. Yu, T.H. Wang, *Electrochim. Acta*, 53 (2008) 8149.
38. M.T. Demirkan, L. Trahey, T. Karabacak, *Thin Solid Films*, 600 (2016) 126.

39. Yu. E. Roginskaya, T. L. Kulova, A. M. Skundin, M. A. Bruk, E. N. Zhikharev, V. A. Kal'nov, *Russian Journal of Electrochemistry*, 44 (2008) 99.